

Electronic Supplementary Information

Glycine-Mediated Surface Stabilization of Amorphous Calcium Phosphate Nanoparticles for Biointeractive Thin-Film Formation

Yuhi Kinoshita,^a Daichi Noda,^{a,b} Zizhen Liu,^{a,c} and Motohiro Tagaya^{a,*}

^a *Department of Materials Science and Bioengineering,
Graduate School of Engineering, Nagaoka University of Technology,
1603-1 Kamitomioka, Nagaoka 940-2188, Japan.*

^b *Japan Society for the Promotion of Science (JSPS) Research Fellowship for Young Scientists (DC),
5-3-1 Koji-machi, Chiyoda-ku, Tokyo 102-0083, Japan.*

^c *Department of Materials Science and Engineering,
School of Materials and Chemical Technology, Institute of Science Tokyo,
4259 Nagatsuta-cho, Midori-ku, Yokohama 226-8501, Japan.*

*** Author to whom correspondence should be addressed:**

Tel: +81-258-47-9345; Fax: +81-258-47-9300, E-mail: tagaya@mst.nagaokaut.ac.jp

Fig. S1

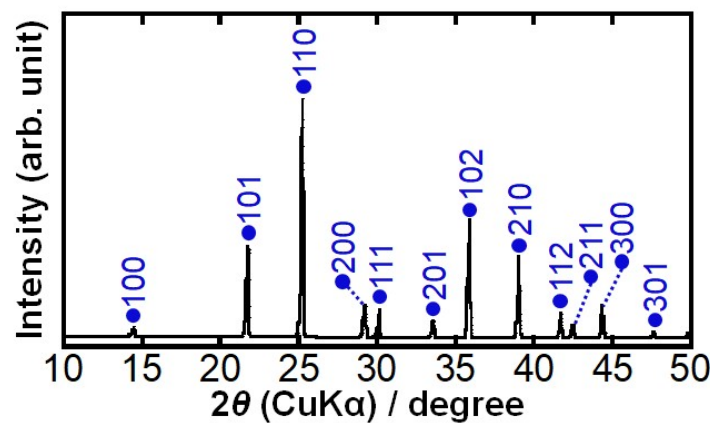


Fig. S1. XRD pattern of γ -Gly powder (ICDD No.: 00-006-0230).

Experimental Procedure S1

The crystal structures of Gly**X-Y** were analyzed by XRD (SmartLab, Rigaku Corporation) using CuK α radiation ($\lambda = 1.5418 \text{ \AA}$) at 40 kV and 30 mA, with a scan speed of $3.0 \text{ }^\circ \text{ min}^{-1}$, a step size of 0.01 ° , and continuous scan mode. The diffraction peak positions and full widths at half maximum were obtained using the instrument software (SmartLab Studio II, Rigaku Corporation). The crystalline phases were identified according to the ICDD standard database by the Hanawalt method. The profile fitting was carried out using the SmartLab Studio II software package, which refines the crystallographic parameters by least-squares fitting of the theoretical peak profiles to the measured data. The refinement of the diffraction patterns was performed using a pseudo-Voigt function (**Eq. (S1)**).

$$f(x) = A \exp\left(-\frac{(x-B)^2}{C^2}\right) + (1-n) \left(\frac{AC^2}{(x-B)^2 + C^2}\right) \quad (\text{S1})$$

Here, **A** is the peak intensity, **B** is the peak position, and **C** is the peak broadening.

The chemical bonding states of Gly**X-Y** were examined by FT-IR spectroscopy (FT/IR-4600, JASCO Corporation) using the attenuated total reflection (ATR) method. The background spectra were recorded in air over a spectral range of $4000\text{-}400 \text{ cm}^{-1}$, with 128 scans and a resolution of 2.0 cm^{-1} . The obtained spectra were corrected by removing the contributions of atmospheric H_2O and CO_2 and by applying baseline correction over the $4000\text{-}400 \text{ cm}^{-1}$ region.

Experimental Procedure S2

The inclusion amount of Gly in Gly $\mathbf{X-Y}$ was determined colorimetrically by the ninhydrin method.^{S1} 20 mg of Gly $\mathbf{X-Y}$ was dissolved in 20 mL of 0.1 M HNO₃ solution and heated with stirring at 70 °C for 1 h, and the solution pH was adjusted to 6.0 with KOH (1 M). Subsequently, 2.0 mL of the pH-adjusted Gly $\mathbf{X-Y}$ solution was mixed with 1.0 mL of ninhydrin solution (95 mM, Product No. 148-08412, FUJIFILM Wako Pure Chemical Corporation) in dimethyl sulfoxide (Product No. 043-07216, FUJIFILM Wako Pure Chemical Corporation), and the solution was kept standing for 12 h at room temperature.

Then, the solution was measured by UV-Vis (V-750, JASCO Corporation). The ninhydrin-reacted product of Ruhemman's purple exhibits a maximum absorbance at 575 nm, and the calibration curve for Gly was prepared using the absorbance at the same wavelength (**Fig. S2, ESI†**).^{S2} Similarly, the absorbance of the Gly $\mathbf{X-Y}$ solution was measured, and the inclusion amounts of Gly were calculated.

References for this page

- S1. A. C. Stauß, C. Fuchs, P. Jansen, S. Repert, K. Alcock, S. Ludewig and W. Rozhon, *Molecules*, 2024, **29**, 3262.
S2. P. P. Vavaiya, N. J. Malviya, A. A. Alshehri, M. Alqarni and H. L. Varu, *J Mol Struct*, 2026, **1350**, 144034.

Fig. S2

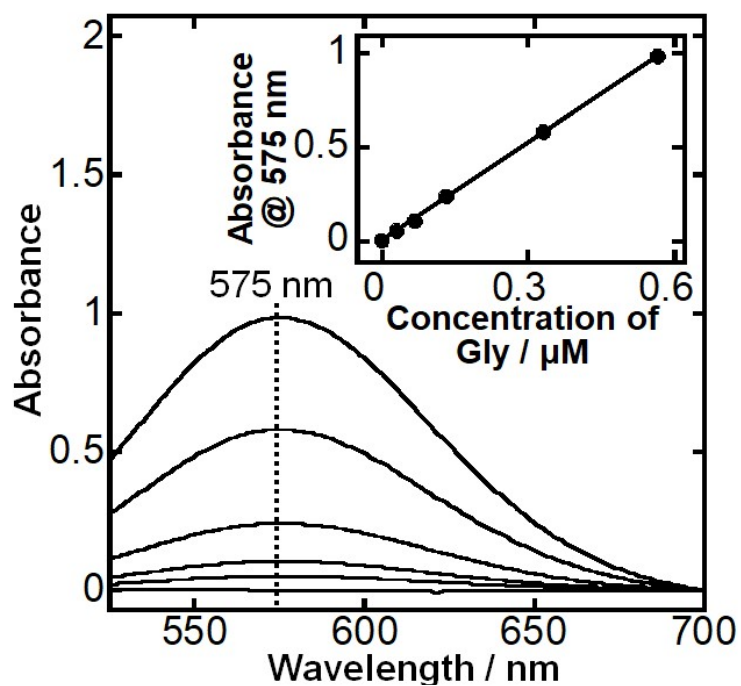


Fig. S2. UV-Vis absorption spectra of Gly aqueous solutions determined colorimetrically by the ninhydrin method. (Inset): the calibration curve between Gly concentration and absorbance ($R^2=0.9997$).

Experimental Procedure S3

The Ca/P and K/Ca molar ratios of Gly \mathbf{X} - \mathbf{Y} were determined by ICP-OES (ICPE-9820, Shimadzu Corporation). 15 mg of the freeze-dried Gly \mathbf{X} - \mathbf{Y} was weighed, dissolved in 10 mL of HNO₃ solution (0.01 M), and then diluted to 50 mL in the volumetric flask. The undissolved residual particles were removed by filtration, and the filtered solution was transferred into the sample holder. The calibration curves of Ca, P, and K ions were constructed using standard solutions of Ca (Product No. 039-16161, FUJIFILM Wako Pure Chemical Corporation), P (Product No. 164-19244, FUJIFILM Wako Pure Chemical Corporation), and K (Product No. 165-17471, FUJIFILM Wako Pure Chemical Corporation), and each diluted solution with 0.002 M HNO₃ solution was used for the measurement. For the quantitative analyses of the molar ratios (Ca/P and K/Ca), the emission wavelengths of Ca at 317.9 nm, P at 213.6 nm and K at 766.5 nm were used.

The Cl/Ca molar ratio of Gly \mathbf{X} - \mathbf{Y} was determined by XRF (ZSX Primus II, Rigaku Corporation). The samples were analyzed without dilution by pressing them into pellets. During the measurement, neither primary filters nor calibration curves were used; instead, the semi-quantitative analysis was performed using the built-in measurement program (EZ scan program, Rigaku Corporation).

Experimental Procedure S4

The nanoparticle shape characterization was performed using a TEM (HT7700, Hitachi High-Tech Corporation) at 100 kV. The samples for the observation were prepared by diluting Gly~~X~~-~~Y~~ in ethanol at 0.005 wt%, casting the dispersion onto carbon-coated copper grids (Product No. NP-C15, Okenshoji Co., Ltd.) and vacuum-drying for 1 day.

Experimental Procedure S5

The hybrid nanoparticle size distribution of Gly**X-E** was measured by the particle size analyzer (ZETASIZER Pro, Malvern Panalytical Ltd.). Gly**X-E** was dispersed in ethanol at a nanoparticle concentration of $0.5 \text{ mg}\cdot\text{mL}^{-1}$, ultrasonically treated and transferred into a folded capillary cell (Product No. DTS1070, Malvern Panalytical Ltd.). The samples were measured by the dynamic light scattering (DLS) method with the refractive index set to be 1.36, the viscosity to be 1.074 mPa·s, and the accumulations count set to be five. The obtained data were analyzed using the instrument software (ZS XPLOERER, Malvern Panalytical Ltd.) to determine the nanoparticle size distribution.

Experimental Procedure S6

The Zeta potential of Gly**X-E** was measured by the Zeta potential analyzer (ZETASIZER Pro, Malvern Panalytical Ltd.). Gly**X-E** was dispersed in ethanol at a particle concentration of $0.5 \text{ mg} \cdot \text{mL}^{-1}$, ultrasonically treated, and transferred into a folded capillary Zeta cell (Product No. DTS1070, Malvern Panalytical Ltd.). The samples were measured by the M3-PALS method with the refractive index set to 1.36, the viscosity to $1.074 \text{ mPa} \cdot \text{s}$, and the accumulations count set to three. The obtained data were analyzed using the instrument software (ZS XPLOER, Malvern Panalytical Ltd.) to determine the Zeta potential values.

The dispersibility of Gly**0.18-E**–Gly**0.48-E** in ethanol was evaluated. The concentration was adjusted to be $9.0 \text{ mg} \cdot \text{mL}^{-1}$, followed by ultrasonication for 30 min (ASU-6, AS ONE Corporation). The dispersions were transferred into 3.5-mL-disposable-cells (Product No. 1961, Kartell S.p.A) and allowed to stand for 17 h, and the dispersibility was evaluated.

Experimental Procedure S7

The GlyX-E nanoparticles were deposited on QCM-D gold sensors (QSensor QSX 301 Gold, Biolin Scientific AB) by the electrophoretic deposition method.^{S3} The GlyX-E were dispersed in ethanol by ultrasonication and adjusted to a solid phase concentration at 1 wt%. In particular, the sensors were immersed in diluted HCl (aq.) and heated at 80 °C for 30 min, followed by the immersion in a mixed solution of H₂O₂ (5 mL), 25% NH₃ (aq.) (5 mL), and ultrapure water (25 mL), and heated at 80 °C for 5 min. The sensors were rinsed with ethanol, dried by nitrogen gas, and treated with UV/O₃ for 10 min (SKB401Y, ASUMI GIKEN Limited). The cleaned sensor and the aluminum counter electrode were connected as the negative and positive electrodes, respectively. The electrodes (electrode distance: 1 cm) were immersed in the GlyX-E dispersion, and a voltage of 100 V was applied for 1 min to deposit the nanoparticles electrophoretically. The nanoparticle deposition was confirmed as shown in **Fig. S3, ESI†**, and the excess nanoparticles were removed by ultrasonication followed by rinsing with ethanol.

Reference for this page

S3. Y. Zhou, Z. Liu, D. Noda, I. Yamada and M. Tagaya, *ACS Biomater Sci Eng*, 2025, **11**, 1150–1160.

Fig. S3

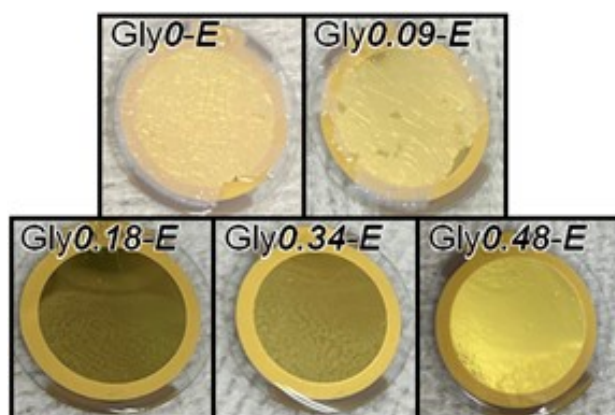


Fig. S3. QCM-D gold sensor images of the deposited GlyX-E before ultrasonic cleaning.

Experimental Procedure S8

The film thickness was evaluated by QCM (Qsense Explorer, Biolin Scientific AB). The deposited weight was calculated by the frequency change (Δf) from the pre- to postdeposition using the Sauerbrey's equation (**Eq. (S2)**)

$$\Delta f = - \frac{2\Delta m n f_0^2}{A \sqrt{\mu_q \rho_q}} \quad (\text{S2})$$

Δf is the frequency change of the crystal oscillator at the 5th harmonic (Hz), f_0 is the fundamental frequency ($f_0 = 15$ MHz), n is the harmonic number ($n = 5$), μ_q is the shear stress of the crystal ($\text{g}\cdot\text{cm}^{-1}\cdot\text{s}^{-2}$), ρ_q is the density of the crystal ($\text{g}\cdot\text{cm}^{-3}$), A is the area of the gold film attached to the crystal plate (cm^2), and Δm is mass of material on the metal film on the crystal surface (g), which is converted to film thickness (nm) using the density of ACP ($2.58 \text{ g}\cdot\text{cm}^{-3}$).^{S4}

Reference for this page

S4. A. Indurkar, R. Choudhary, K. Rubenis, M. Nimbalkar, A. Sarakovskis, A. R. Boccaccini and J. Locs, *ACS Omega*, 2023, **8**, 26782–26792.

Experimental Procedure S9

Surface observation of **GlyX-E (X=0.18–0.48)** was carried out using an atomic force microscope (AFM, NanoNavi II / E-sweep, SII NanoTechnology Inc.) in tapping mode. AFM measurements were performed using a cantilever (SII microcantilever SI-AF01, Hitachi High-Tech Corporation) equipped with a silicon probe. The root-mean-square roughness (R_q (nm)) was calculated using the following **Eq. (S3)**.

$$R_q = \sqrt{\frac{1}{n} \sum_{i=1}^n (h(x_i) - h)^2} \quad (\text{S3})$$

Here, n is the number of measurement points, $h(x_i)$ is the height at the measurement point x_i , and h is the average height. Furthermore, the nanoparticle size distribution was determined from the AFM topographic images by measuring 100 individual particles, from which the average value (Ave.) and coefficient of variation (Cv.) of the nanoparticles were calculated.

Fig. S4

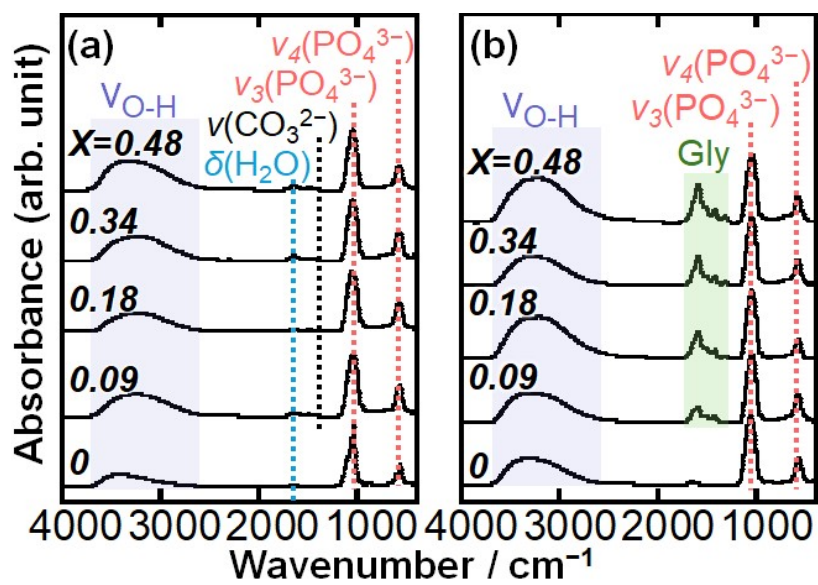


Fig. S4. FT-IR spectra (4000-400 cm⁻¹) of (a) GlyX-W and (b) GlyX-E.

Fig. S5

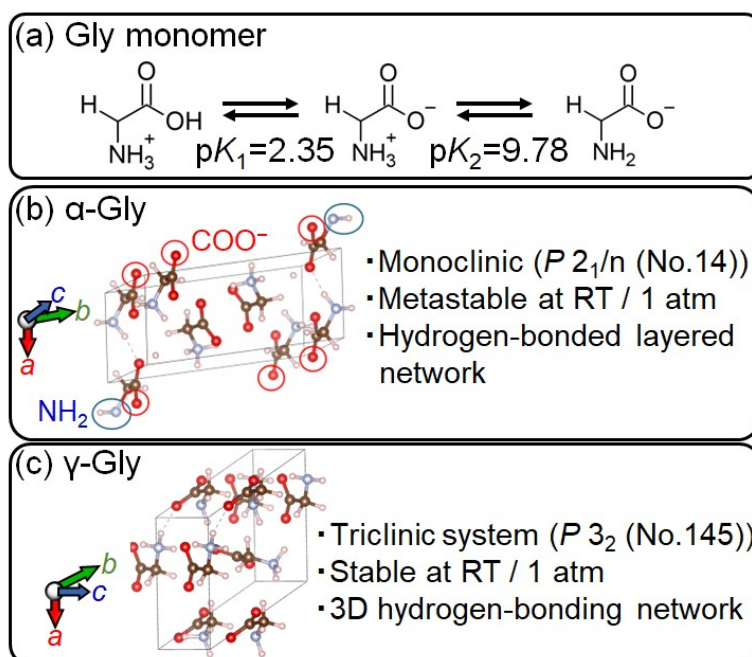


Fig. S5. (a) Dissociative states of Gly monomer, and intermolecular interaction structures of (b) α -Gly and (c) γ -Gly.

Fig. S6

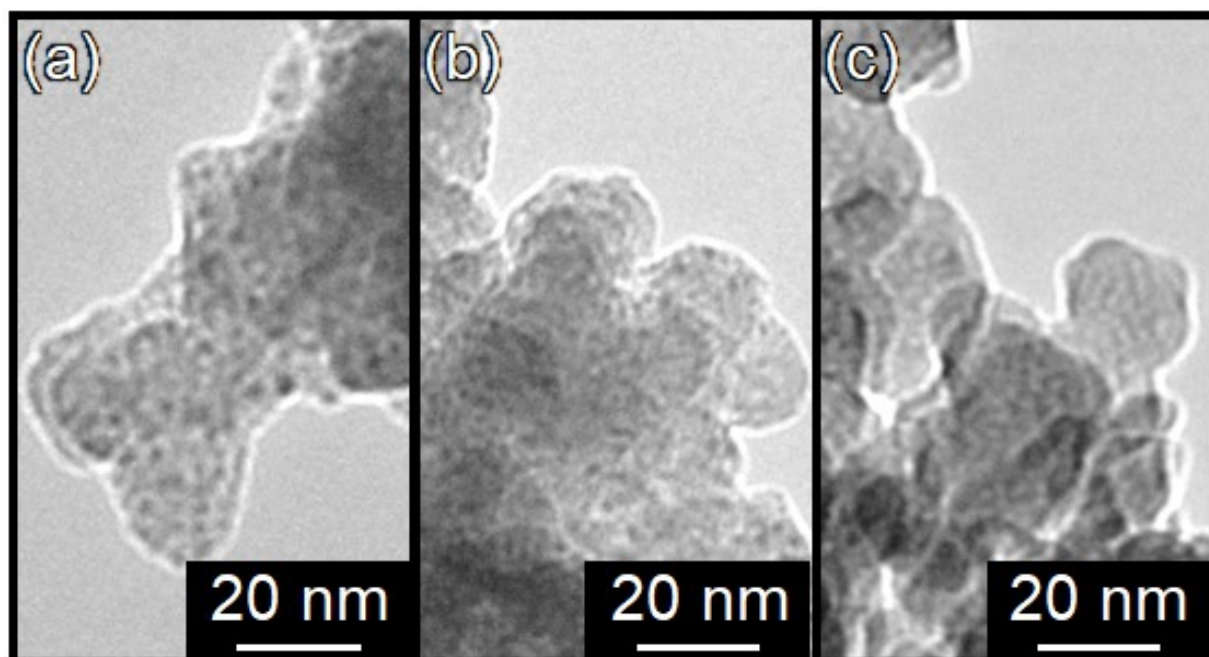


Fig. S6. TEM images of (a) Gly0.18-E, (b) Gly0.34-E and (c) Gly0.48-E.

Fig. S7

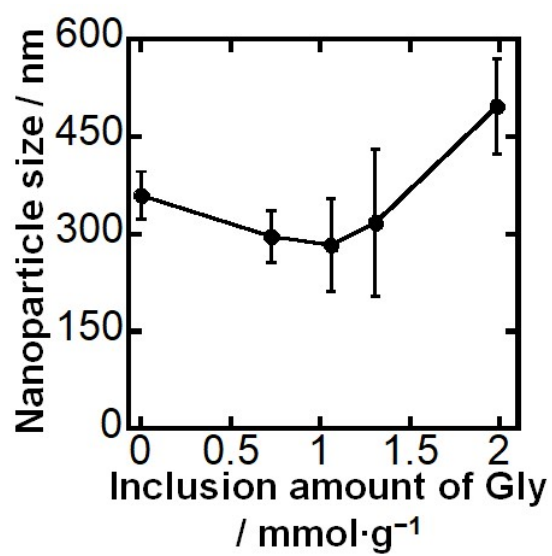


Fig. S7. Change in the hybrid nanoparticle size in ethanol for GlyX-E with the inclusion amount of Gly.

Fig. S8

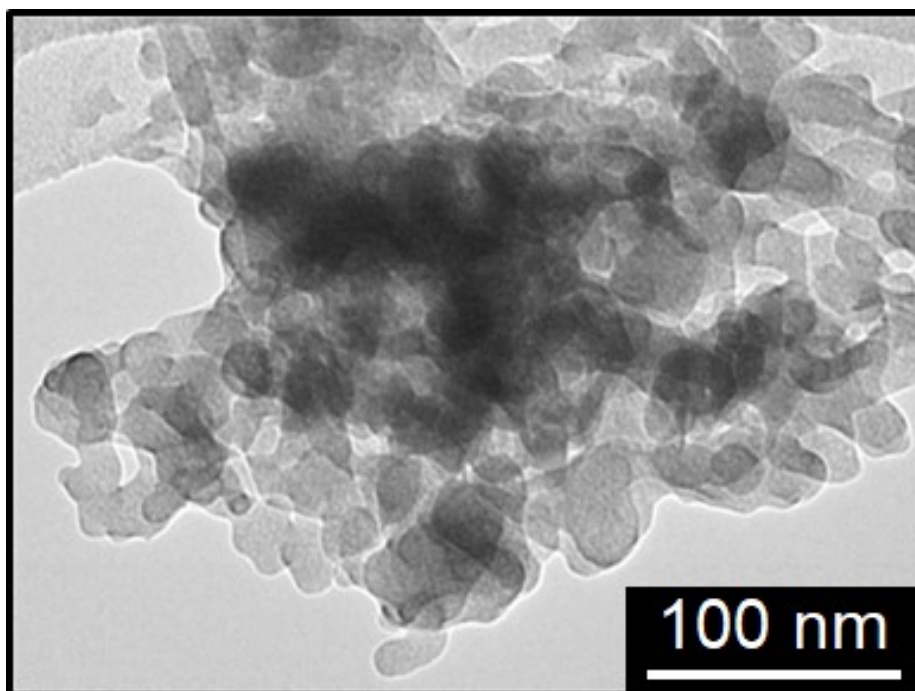


Fig. S8. Representative TEM image of the aggregated hybrid nanoparticle state of Gly0.18-E.

Fig. S9

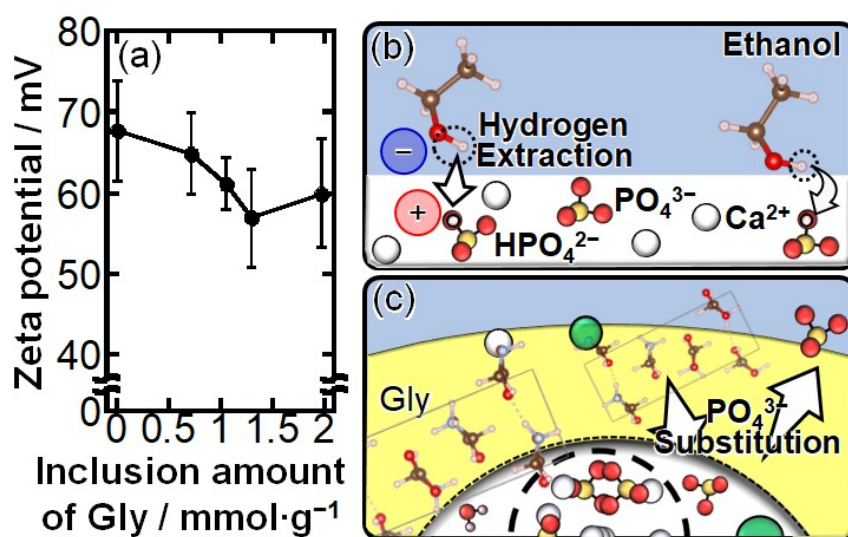


Fig. S9. (a) Change in the Zeta potential of Gly_X-E in ethanol with the inclusion amount of Gly. (b, c) Illustrations of the surface layer states of (b) Gly₀-E and (c) Gly_{0.09}-E–Gly_{0.48}-E.

Fig. S10

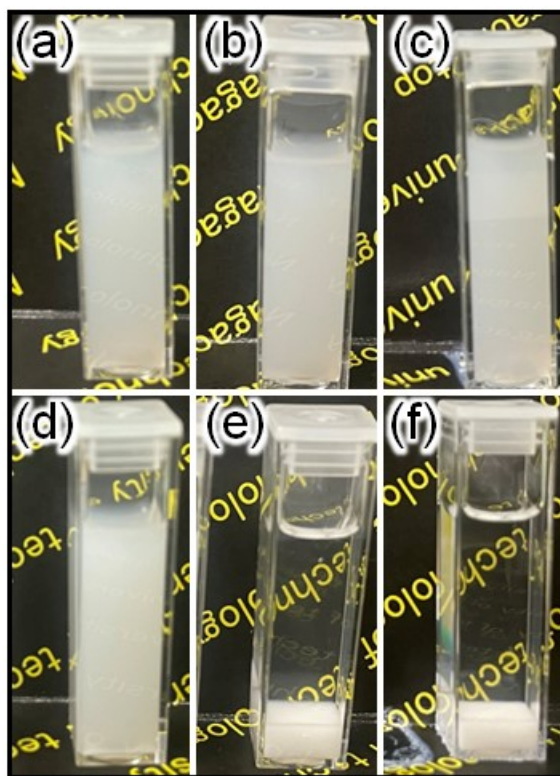
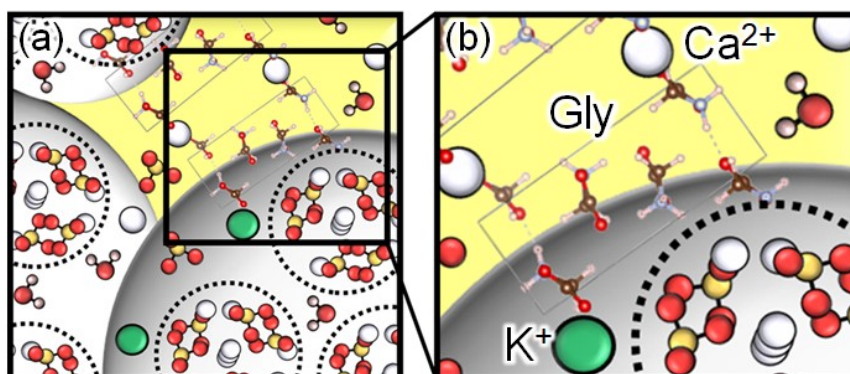


Fig. S10. (a–f) Hybrid nanoparticle dispersion states of: (a, d) Gly $0.18-E$ (b, e) Gly $0.34-E$ (c, f) Gly $0.48-E$ in ethanol (a–c) before and (d–f) after freeze-drying for 17 h.

Scheme. S1



Scheme S1. Illustration of (a) GlyX-E in which the interactions analogous to those in α -Gly are formed on the ACP nanoparticles, and (b) the enlarged view of the surface.

Fig. S11

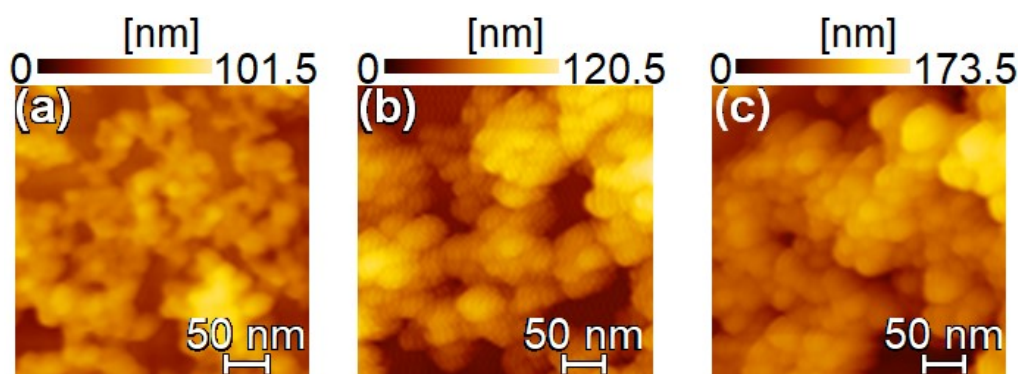


Fig. S11. Magnified AFM topographic images of (a) Gly**0.18-E**, (b) Gly**0.34-E** and (c) Gly**0.48-E**.